MASSIVE STAR FORMATION IN THE INFRARED-BRIGHT GALAXY NGC 972

SWARA RAVINDRANATH AND TUSHAR P. PRABHU

Indian Institute of Astrophysics, Koramangala, Bangalore 560 034, India; cathy@iiap.ernet.in, tpp@iiap.ernet.in

ABSTRACT

We present the results of optical broadband and Hα imaging studies of the infrared-bright galaxy NGC 972. The broadband images and B/R color map reveal the peculiar morphology and complex dust distribution. Massive star formation activity in this galaxy is evident from the continuum-subtracted Hα image, which shows the presence of circumnuclear activity and disk star formation within a radius of 3.4 kpc. The circumnuclear star-forming regions are distributed in a ring of radius 630 pc and closely associated with an inner dust ring. Aperture photometry has been performed on the individual H II regions, and we estimate an age ≤ 5.4 Myr for the nuclear starburst using evolutionary synthesis models. The Hα luminosity of the nucleus is comparable to that of starburst nuclei. The emission-line ratios of NGC 972 are also indicative of a nuclear starburst, which is powered by photoionization by a large number of hot, massive stars. The enhancement of low-ionization lines compared with normal H II regions can be attributed to the influence of dust on the thermal properties of the nebula or to contributions by shocks from supernova remnants. The star formation rate is estimated as 0.32 $M_{\odot}$ yr^{-1} for the nucleus and 2.1–2.7 $M_{\odot}$ yr^{-1} in the inner 3.6 kpc of the galaxy.

Key words: galaxies: individual (NGC 972) — galaxies: starburst — H II regions — stars: formation

1. INTRODUCTION

The northern galaxy NGC 972, also known as UGC 2045, is remarkable for its chaotic dust distribution in the main body, which makes it similar in appearance to the prototype starburst galaxy, M82. De Vaucouleurs et al. (1991, hereafter RC3) classify it as morphological type Sab, and in the Revised Shapley-Ames Catalog by Sandage & Tammann (1987), it has been classified as Sb pec. It is interesting to note that NGC 972 was classified as I0 in the Second Reference Catalogue of Bright Galaxies by de Vaucouleurs, de Vaucouleurs, & Corwin (1976) and has often been listed in the class of M82-type galaxies (Andreasian & Khachikian 1979; Burbidge, Burbidge, & Prendergast 1965). The bright main body of the galaxy exhibits very complicated dust patterns, and deep images reveal the outer regions with a much fainter and smooth light distribution. From the RC3, the heliocentric and Galactic standard of rest–relative systemic velocities are 1543 and 1640 km s^{-1}, respectively, yielding an estimated distance of 21.9 Mpc for the galaxy (using $H_0 = 75$ km s^{-1} Mpc^{-1}). At this distance, $1''$ corresponds to 105 pc.

Condon & Broderick (1988), Young et al. (1989), and Spinoglio & Malkan (1989) give a good compilation of the radio and infrared properties of NGC 972. Interesting correlations of the *IRAS* 40–120 μm luminosity with the molecular gas mass and Hα luminosity for spiral galaxies support the view that a major contribution to the far-infrared (FIR) luminosity is the thermal emission from dust heated by massive stars. Hence, the $L(40–120$ μm) luminosities are used to quantify massive star formation rates. NGC 972 belongs to the list of early-type spiral galaxies with the highest FIR luminosities [$L(40–120$ μm) $\geq 10^{10}$ $L_{\odot}$] compiled by Devereux & Hameed (1997). Like most of the galaxies belonging to this list, NGC 972 reveals huge complexes of H II regions in the Hα images, which are hidden from view in the continuum images because of the dominant stellar bulge. Condon & Broderick use the FIR-to-radio flux density parameter (u) and the infrared

spectral index α_{IR} to identify the energy source. They conclude that the radio and infrared emission seen in NGC 972 is powered by a starburst. The L_{IR}/L_B ratio is 2.02, and log $L(40–120$ μm) = 10.43 $L_{\odot}$; these high values support the starburst nature of NGC 972 since they imply the presence of a recent burst of formation of massive stars.

The total blue magnitude (B_T), corrected for Galactic and internal absorption, is 11.46 (Tully 1988), and the corresponding blue luminosity in solar units is given by log $L_B = 10.27$. Previous studies, involving a photometric investigation of NGC 972, show that half of the light of this galaxy is concentrated within a radius of $35''$ (Andreasian & Khachikian 1979). Vennick & Richter (1994) analyzed the B-band surface brightness profile and found that the brightness distribution can be approximated by two exponentials and the change in the profile toward the outer regions indicates the presence of a halo component. Hodge & Kennicutt (1983) mention the identification of 13 H II regions in NGC 972 while presenting their atlas of H II regions in galaxies. Spectroscopic studies of NGC 972 have been carried out by Andreasian & Khachikian (1979), Taniguchi (1986), and Ho, Filippenko, & Sargent (1995) with a view to establishing the nature of the nuclear activity. All these studies have emphasized the presence of a strong continuum and an emission-line spectrum typical of gaseous nebulae. Since the Hα + [N II] emission lines are strong throughout the main body of the galaxy, Burbidge et al. (1965) used these intense emission lines to obtain the rotation curve of NGC 972. They estimate a mass of 9×10^9 $M_{\odot}$ interior to $36''$, and the total mass of the galaxy is estimated to be 1.3×10^{10} $M_{\odot}$ (Burbidge et al. 1965; Roberts 1969). The mass of neutral hydrogen within the galaxy is 1.05×10^9 $M_{\odot}$ (Tully 1988).

The present work provides the results of an optical broadband and Hα emission-line imaging study of NGC 972, with an aim to understanding the photometric properties and evolution of the star-forming regions using evolutionary synthesis models. Based on the Hα fluxes that we

derive and other information available in the literature, we discuss the nature of the ionizing source that powers the nuclear emission-line spectrum of NGC 972, emphasizing its similarities with other classical starburst galaxies.

2. OBSERVATIONS AND REDUCTIONS

Broadband BVR images and narrowband $H\alpha$ (100 Å) images were obtained on 1996 November 5 and 6 using the 2.34 m Vainu Bappu Telescope equipped with a 1024×1024 pixel Tektronix CCD. The image scale at the prime focus corresponds to $0\rlap{.}''6$ pixel^{-1}, and the CCD covers a field of $10' \times 10'$ on the sky. Exposure times and other observational details are summarized in Table 1. The Landolt standard star field PG 0231+051 (Landolt 1992) was observed for local atmospheric extinction correction. The spectrophotometric standard star PG 0310+149 from Massey et al. (1988) was observed in the R band as well as the $H\alpha$ band for flux calibration.

Bias subtraction and flat-fielding were performed using the standard package CCDRED under the IRAF[1] image reduction software. After cosmic-ray removal, the frames were aligned through a geometric mapping using the GEOTRAN and GEOMAP tasks available in the reduction software. The transformed star positions agreed to within 0.3 pixels as judged from the coordinates of common stars in different frames.

The $H\alpha$ images contain a significant amount of the red continuum that passes through the 100 Å passband of the $H\alpha$ filter. The subtraction of the continuum contribution to the $H\alpha$ band was done by following the method described by Waller (1990). The sky level was estimated from the R and $H\alpha$ images and subtracted. The scaling factor between the R and $H\alpha$ bands was determined using the foreground stars in the field of the galaxy. Aperture photometry of the individual H II regions identified on the pure emission-line image was performed using the APPHOT package in IRAF. After sky subtraction from the broadband and $H\alpha$ frames, the underlying galaxy background was estimated by defining rectangular apertures on either side of the circular apertures enclosing the individual H II regions. The mean background value from the rectangular apertures adjacent to the H II region of interest was subtracted from the counts within the H II region aperture. The nonuniformity of the galaxy background can introduce considerable errors in the photometry, particularly for the H II regions lying near the bulge of the galaxy. Also, the circular apertures chosen for the individual H II regions sample only the core of the emission region, even though the actual emission extends beyond our apertures. We used similar apertures for most of the H II regions, typically $3''-4''$. Hence some of the large H II regions may be undersampled, and the $H\alpha$ fluxes given in this work are only lower limits. The results of the aperture photometry are given in Table 2. Photometry of the galaxy was also performed using the same apertures given in Longo & de Vaucouleurs (1983). We find that our photometric errors are about 0.008 mag in V and 0.04 mag in $B-V$.

3. RESULTS

3.1. Broadband Imaging

On the broadband images, NGC 972 exhibits a very peculiar morphology with complex dust distribution (see Fig. 1). The images reveal a bright nucleus and main body up to a radius of $35''$. Beyond this radius, the outer regions of the galaxy exhibit a fainter and almost featureless light distribution. The inner regions are traversed by a number of dust lanes, and this enormous amount of dust, distributed in a random fashion, gives NGC 972 the appearance of an irregular galaxy. The broadband images also show a very bright knot located about $12''$ north of the nucleus, which emits strongly in the continuum and appears as bright as the nucleus itself. Since the B image, which samples the young hot stars and ionized gas, is more severely affected by the obscuring effects of dust compared with the R image, which samples the underlying stellar population, B/R color maps can be used to emphasize the anomalous dust distribution. The B/R map is shown in Figure 2. The nucleus is surrounded by dust, which forms a ring with a radius of about 630 pc. This is very similar in appearance to the circumnuclear dust ring seen in the color map of NGC 7552 (Forbes et al. 1994, their Fig. 5). On the far side of the nucleus, short plumes of dust are faintly visible in the original image, emanating from the dust ring, toward the northeast direction. Vertical dust filaments and plumes emanating from actively star-forming regions are common in galaxies, and more evident for galaxies with high inclinations. The dust plumes of NGC 972 are not as prominent as in the case of NGC 1808 (Phillips 1993), and it is not clear whether they are off-planar structures. Two prominent dark lanes, which lie along the northwest arm and the southeast arm, roughly trace the spiral structure of the galaxy. These two arms clearly delineate the bright inner region and the faint outer region. Even though the dust appears to be very chaotic on the near side, the two prominent arms close into a ring on the farther side. Comparing with the $H\alpha$ images, it is found that this outer ring encloses all the star-forming knots. Also, it is clear that the dust distribution within this region is closely associated with the distribution of H II regions. The inner dust ring surrounding the nucleus causes severe obscuration of the circumnuclear H II regions. The bright knot seen north of the nucleus on broadband images appears quite blue in the color map. From the dust distribu-

TABLE 1
SUMMARY OF OBSERVATIONS

Filter	$\lambda/\delta\lambda$ (Å)	Exposure Time (s)
1996 Nov 5:		
B	4400/1050	300
V	5425/1050	300
R	6550/1300	600
$H\alpha$	6581/100	1500
1996 Nov 6:		
B	4400/1050	900
V	5425/1050	600
R	6550/1300	900
$H\alpha$	6581/100	1200

NOTES.—Observations obtained with the 2.34 m Vainu Bappu Telescope equipped with a 1024×1024 Tektronix CCD. The image scale was $0\rlap{.}''6$ pixel^{-1}, and the seeing was $1\rlap{.}''8$ and $2\rlap{.}''0$ on November 5 and 6, respectively.

TABLE 2

RESULTS OF APERTURE PHOTOMETRY OF H II REGIONS

Region	Aperture Radius (arcsec)	V	$B-V$	$V-R$	$\log F_{H\alpha+[NII]}$	$W(H\alpha + [N\ II])$ (Å)
k1	1.8	20.54	0.71	0.87	−13.64	618.6
k2	1.8	20.28	0.69	0.76	−13.61	585.0
k3	2.4	18.31	0.78	0.61	−13.44	163.0
k4	1.8	18.15	0.68	0.51	−13.64	96.5
k5	1.8	20.25	1.15	0.89	−13.87	274.43
k6	1.8	18.09	0.97	0.61	−13.97	38.93
k7	1.8	18.36	0.62	0.48	−13.59	134.8
k8	1.8	17.77	0.73	0.49	−13.64	68.37
k9	1.8	18.83	1.07	0.84	−13.82	89.23
k10	1.8	16.61	0.96	0.66	−12.98	93.63
k11	1.8	19.05	1.36	0.93	−13.67	138.2
k12	1.8	18.16	1.37	0.88	−13.67	65.172
k13	1.8	18.71	0.77	0.60	−13.70	128.9
k14	1.8	17.62	0.85	0.56	−13.85	34.40
k15	2.4	16.78	0.66	0.51	−12.79	194.5
k16	1.8	19.28	0.97	0.91	−13.42	310.4
k17	1.8	18.25	0.34	0.34	−13.52	163.4
k18	1.8	18.22	0.74	0.65	−13.29	201.4

tion, it appears that the southwest side of NGC 972 is the near side.

3.2. Hα Imaging

Hα imaging effectively traces the distribution of gas photoionized by young OB stars and, thereby, the sites of recent massive star formation. The continuum-subtracted emission-line image is shown on a gray scale in Figure 3a, and the contour plot is given in Figure 3b. Current star formation in NGC 972 is evident from this image, which reveals a number of bright, star-forming knots in the nuclear, circumnuclear, and disk regions. All the Hα knots are confined within a radius of 3.4 kpc. In the continuum image the star-forming regions are hidden from view by the
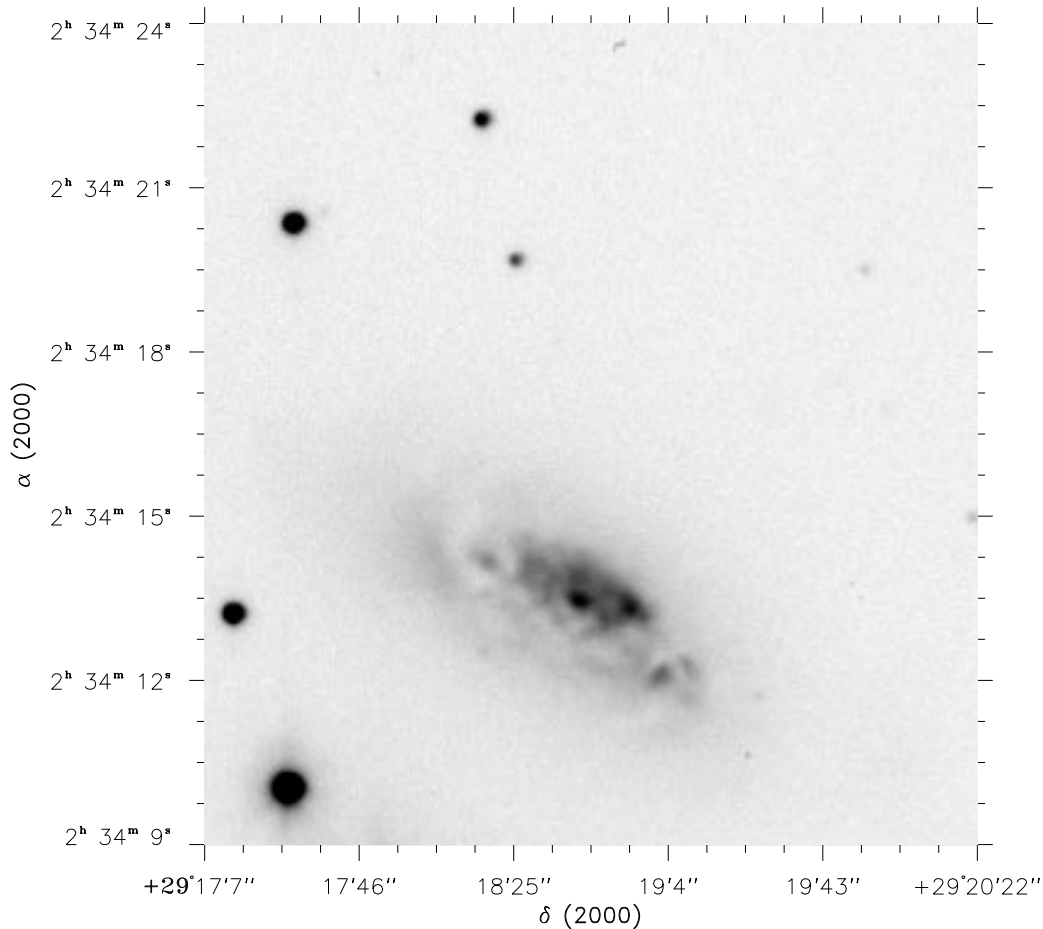

FIG. 1.—Broadband B image, revealing the peculiar morphology of NGC 972. North is to the right, and east is to the top. The total field is 3′.25 × 3′.25.
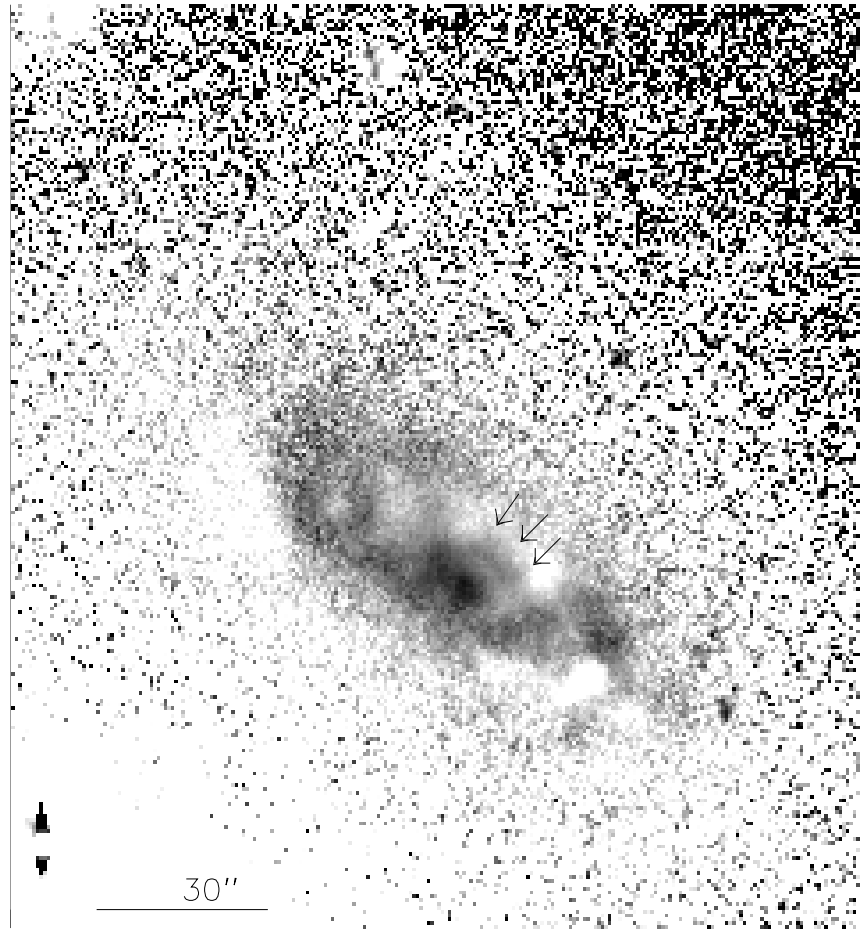
Fig. 2.—B/R color map, emphasizing the complex dust distribution in the main body of NGC 972. North is to the right, and east is to the top. The arrows point toward the location of diffuse plumelike structures mentioned in the text. The total field is $2'.5 \times 2'.5$. The red regions appear dark, and blue regions appear light.

bright stellar bulge, as in the case of most early-type galaxies, like NGC 3504, 1022, 2782, and 7552 (Devereux & Hameed 1997). When the dominant contribution from the stellar bulge is subtracted, the star formation activity becomes evident. The Hα knots in the circumnuclear region form a partial ring of radius 630 pc, with a break southeast of the nucleus. There are five Hα knots (indicated in Fig. 3a as k9, k11, k12, k13, and k14) that form the partial ring

TABLE 3

PROPERTIES OF INDIVIDUAL H II REGIONS

Region	R.A. (J2000.0)	Decl. (J2000.0)	V	$B-V$	$V-R$	$\log F_{\mathrm{H}\alpha}$	$\log L_{\mathrm{H}\alpha}$	$\log N_{\mathrm{Lyc}}$
k1	2 34 13.51	29 18 19.14	18.64	0.07	0.38	−13.33	39.40	51.26
k2	2 34 13.33	29 18 24.21	18.38	0.07	0.27	−13.29	39.43	51.30
k3	2 34 14.02	29 18 21.21	16.41	0.15	0.12	−13.12	39.61	51.47
k4	2 34 14.14	29 18 29.52	16.25	0.05	0.02	−13.32	39.41	51.27
k5	2 34 12.94	29 18 31.12	18.35	0.52	0.40	−13.55	39.17	51.04
k6	2 34 14.06	29 18 37.13	16.19	0.34	0.12	−13.66	39.07	50.93
k7	2 34 14.28	29 18 44.09	16.46	−0.01	−0.01	−13.33	39.40	51.26
k8	2 34 13.88	29 18 50.16	15.87	0.10	0.01	−13.33	39.40	51.26
k9	2 34 13.55	29 18 47.93	15.49	−0.02	−0.03	−13.06	39.66	51.53
k10	2 34 13.45	29 18 42.33	13.27	−0.13	−0.20	−12.23	40.50	52.37
k11	2 34 13.23	29 18 36.73	15.71	0.27	−0.07	−12.92	39.81	51.68
k12	2 34 13.13	29 18 39.77	14.83	0.27	−0.02	−12.91	39.81	51.68
k13	2 34 12.91	29 18 45.51	15.37	−0.32	−0.26	−12.95	39.78	51.64
k14	2 34 13.20	29 18 48.92	14.28	−0.25	−0.30	−13.10	39.62	51.49
k15	2 34 13.25	29 18 59.19	14.88	0.03	0.02	−12.47	40.26	52.12
k16	2 34 12.48	29 18 56.66	17.38	0.34	0.42	−13.11	39.62	51.48
k17	2 34 12.26	29 19 03.58	16.35	−0.29	−0.15	−13.20	39.52	51.39
k18	2 34 12.39	29 19 09.01	16.32	0.11	0.16	−12.98	39.75	51.62

NOTE.—Units of right ascension are hours, minutes, and seconds, and units of declination are degrees, arcminutes, and arcseconds.
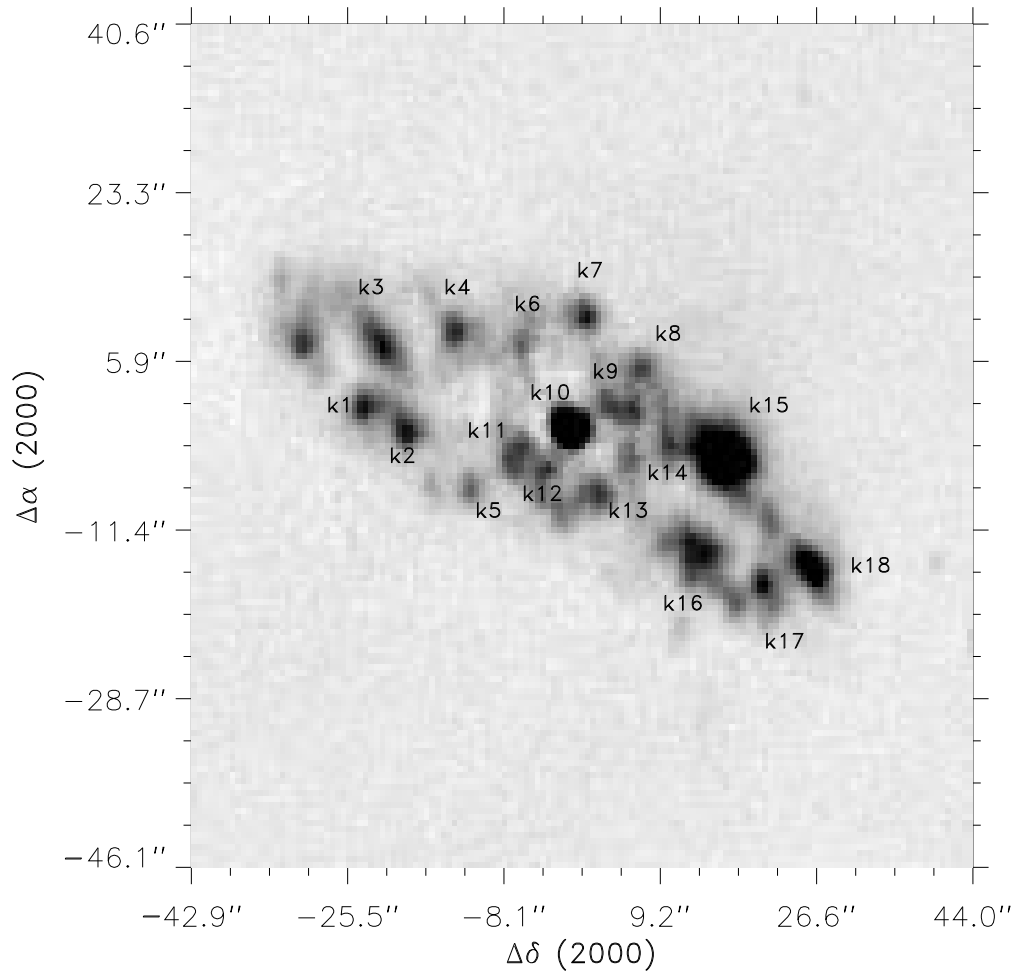
FIG. 3a

FIG. 3.—(a) Continuum-subtracted Hα image of NGC 972, revealing the distribution of star-forming regions. The H II regions for which photometry has been performed are marked. The unmarked H II region at the extreme south has not been used in the analysis, since it is too faint in the continuum images. The total field shown here is 1'.4 × 1'.4. The axes are marked in arcseconds with reference to the nucleus at (0, 0). (b) Contour plot of the continuum-subtracted Hα image. The axes are in pixel units and the region covers 1'.6 × 1'.4.

around the nucleus (k10), while the remaining knots belong to the disk. A comparison of the broadband images and emission-line image shows that the regions that are bright in the continuum are spatially separated from the regions that are bright in the emission-line image. There is a very prominent H II region in the continuum-subtracted Hα image that lies about 16″ north of the nucleus and is close to the brightest continuum knot seen in broadband images. This giant H II region (labeled k15 in Fig. 3a) has extended emission and appears as luminous as the nucleus on the emission-line image, much like the "jumbo" H II region of NGC 3310 (Balick & Heckman 1981). We have identified 19 H II regions and performed aperture photometry on them as described in § 2. The Hα + [N II] fluxes and equivalent widths given in Table 2 were calculated using the expressions for line fluxes and equivalent widths given by Waller (1990).

The equatorial coordinates for 12 stars seen in our images were obtained from the *Hubble Space Telescope* Guide Star Catalog. Using this information, astrometry was performed for the H II regions. The results are given in Table 3. Knowing the position angle and inclination of the galaxy from the RC3, a deprojection of the coordinates was done in order to visualize the distribution of H II regions in

the plane of the galaxy. It is seen that the circumnuclear knots are contained within an elliptical ring whose major axis is aligned perpendicular to the line of nodes of the galaxy. The deprojected semimajor axis of the circumnuclear ring comes to about 1 kpc. Though the distribution of the knots is chaotic, it is possible to trace out two spiral arms formed by the disk H II regions.

4. DISCUSSION

4.1. *Star Formation History*

Evolutionary population synthesis models aim at deriving the observable properties of a population of stars at different times of its evolution. Models for stellar atmospheres and stellar evolution are used to predict the emergent spectrum and other observable parameters for a chosen initial mass function (IMF). Hence, the age of the stellar population can be estimated by comparing the observed quantities with those predicted by the synthesis models.

Before comparing the observables with models, corrections have to be made for interstellar reddening, which arises from three sources—the interstellar medium (ISM) of our Galaxy, the ISM of the parent galaxy, and the dust
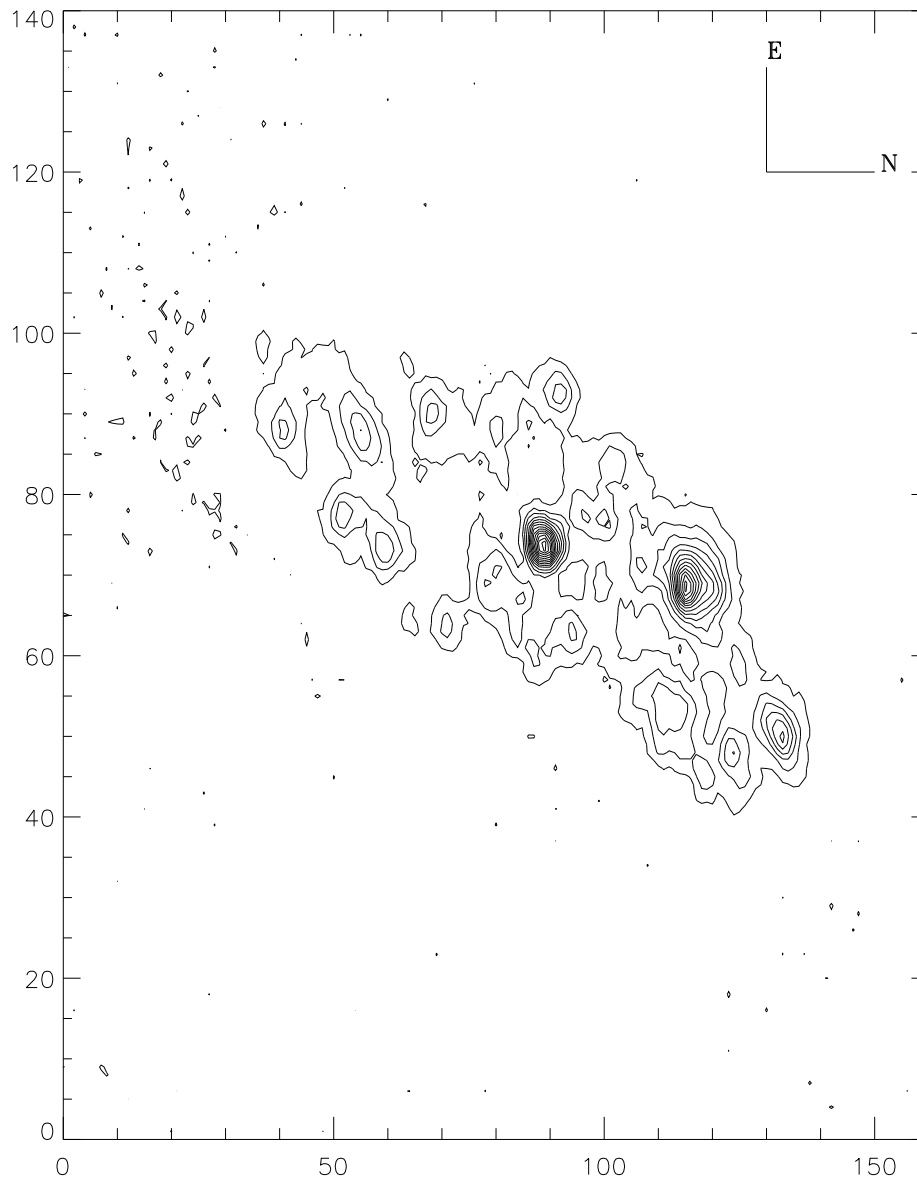
FIG. 3b

mixed with gas within the H II region. For NGC 972, the Galactic extinction in the broad bands was obtained using $A_B = 0.37$ from the RC3 and the extinction law from Cardelli, Clayton, & Mathis (1989) with $R_v = 3.1$. For the internal extinction within the parent galaxy, a value of $A_B^i = 0.36$ taken from the RC3 was used; this also includes a correction for inclination. The spectroscopic ratio Hα/Hβ yields an estimate of the Balmer decrement, which is used to determine the visual extinction A_v within the H II regions. L. C. Ho (1997, private communication) gives Hα/Hβ as 7.7 for the nucleus of NGC 972, which corresponds to an A_v of 2.8 mag. A recent study of H II regions in the centers of nearby galaxies carried out by Ho, Filippenko, & Sargent (1997) yielded a median internal reddening of $E(B-V) = 0.54$, using the Balmer decrement for early-type spiral galaxies (S0 to Sbc). Assuming the Galactic extinction law ($R_v = 3.1$), this implies a visual extinction of $A_v = 1.67$. Thus the nuclear extinction in NGC 972 is higher than the median value of extinction for early-type spirals even after correcting for inclination effects, which account only for 0.4 mag.

The observed Hα fluxes are contaminated by the presence of strong [N II] lines at 6548 and 6583 Å, which fall within the 100 Å–wide Hα filter. The pure Hα fluxes are obtained from the observed Hα + [N II] fluxes by assuming a value of Hα/(Hα + [N II]) = 0.70 based on the spectroscopic data for the nucleus from L. C. Ho (1997, private communication). This agrees with the value of 0.72 given by Kennicutt (1983) for typical H II regions. The Hα luminosities derived from the fluxes can be used to estimate the current star formation rate by computing the number of Lyman continuum photons that are being emitted by massive stars in the ionization-bounded H II regions. If all of the Lyman continuum photons are absorbed in the photoionization, then for case B recombination with $T_e = 10,000$ K, the number of Lyman continuum photons is related to the Hα luminosity by

$$N_{\mathrm{Lyc}} = 7.34 \times 10^{11} L(\mathrm{H}\alpha) \text{ photons s}^{-1} ,$$

where $L(\mathrm{H}\alpha)$ is the luminosity in ergs s^{-1} (Kennicutt 1983).

Table 3 gives the extinction-corrected colors and Hα

fluxes (free from [N II] contamination), Hα luminosities, and the number of Lyman continuum photons. The colors and fluxes given in the table were obtained by using the Balmer decrement estimate of $A_v = 2.8$ mag to obtain the internal reddening in the nuclear and circumnuclear regions, and using $A_v = 1.3$ mag, which is the typical average extinction for optically selected giant H II regions in spiral galaxies (Kennicutt 1988), to estimate the internal reddening in the disk H II regions. The number of Lyman continuum photons emitted by an O5 star is of the order of 10^{49} photons s^{-1}. Hence the number of ionizing O5 stars required in individual H II regions of NGC 972 corresponds to 100–1000 stars. As seen from the table, most of the H II regions have Hα luminosities that are typical of giant extragalactic H II regions (GEHRs), being in the range of 10^{39} to 10^{40} ergs s^{-1}. The nucleus and the most prominent H II region have luminosities comparable to starburst galaxies, with log L(Hα) of 40.50 and 40.26, respectively. The number of ionizing photons in the nucleus is given by log $N_{\mathrm{Lyc}} = 52.4$, implying the presence of 1000 O5 stars. For comparison, in the case of the starburst region 30 Doradus, in the LMC, log N_{Lyc} is about 52, for a log L(Hα) of 40.2 (Conti 1991). Table 4 gives the estimates of star formation rate (SFR) for four of the brightest H II regions in NGC 972 calculated from the Hα luminosities, following Kennicutt (1983). The SFR is given by the expressions

$$\mathrm{SFR}(\geq 10\ M_\odot) = \frac{L(\mathrm{H}\alpha)}{7.02 \times 10^{41}\ \mathrm{ergs\ s}^{-1}}\ M_\odot\ \mathrm{yr}^{-1},$$

$$\mathrm{SFR(total)} = \frac{L(\mathrm{H}\alpha)}{1.12 \times 10^{41}\ \mathrm{ergs\ s}^{-1}}\ M_\odot\ \mathrm{yr}^{-1}.$$

The observed parameters given in Table 3 have been compared with the parameters predicted from the evolutionary synthesis model of Mayya (1995) for an instantaneous burst characterized by a Salpeter IMF with $M_{\mathrm{up}} = 100$ $M_\odot$, $M_{\mathrm{low}} = 1\ M_\odot$, and slope $\alpha = 2.35$, at solar metallicity. The large uncertainties in the internal reddening within the H II regions make it difficult to infer the ages of these regions based on the colors. Hence, we have used two different approaches to estimate the ages. In one approach, we used a value of $A_v = 2.8$ obtained from the Balmer decrement seen in the nuclear spectra, for correcting for the internal extinction in the nuclear and circumnuclear star-forming knots. The disk regions were corrected using a value of $A_v = 1.3$ mag, corresponding to the typical extinction of 1.1 mag at Hα given by Kennicutt (1988) for the H II regions in spiral galaxies. These extinction corrections resulted in colors (see Table 3) that were too blue compared with the model colors and were inconsistent with the ages implied by the measured Hα equivalent widths. The extreme blue colors for the nucleus after correction for reddening (using the Balmer decrement obtained from nuclear spectroscopic ratios) probably imply a different extinction for

the stellar and nebular components, as found in several other galaxies. There has been evidence for selective obscuration due to patchy dust distributions in H II regions. The extinction effects of such clumpy dust may be different for stars and ionized gas (Keel 1993; Mayya & Prabhu 1996; Calzetti, Kinney, & Storchi-Bergmann 1994). Mayya & Prabhu (1996) found that dereddening the stellar observed quantities by the extinction derived from Balmer decrement results in an overcorrection for extinction toward the stellar component. They inferred that the stellar continuum on average experiences lesser extinction than the nebular continuum, which would be the case if the dust distribution was patchy and the radiation from the ionized gas was selectively absorbed by the dust. Calzetti et al. (1994) refer to the discrepancy between the value of extinction obtained from the UV continuum and Balmer line ratios for their sample of starburst galaxies. In their attempt to derive an effective extinction law, they find that the difference between the optical depths of the continuum underlying the Balmer lines is about one-half of the difference between the optical depths of the Balmer emission lines.

In our second approach, we grouped the H II regions into three classes based on their location amid the complex dust lanes, which cause nonuniform extinction. The B/R color map, which reveals the dust morphology, was used for this purpose, with the H II region apertures superposed on it. Assuming that the equivalent width is not much affected by the extinction, we used the equivalent width of Hα versus $B-V$ diagrams to obtain an estimate of $E(B-V)$, which would give the color excess over that predicted by the model for the age implied by the equivalent width. It is found that knots k1, k2, k5, k9, k11, k12, k16, and k18, all of which lie closely associated with dust lanes, have higher average extinction, with $A_v = 3.1$. From their location on the dust map, it is evident that all these knots are on the near side of the galaxy and are seen through the dust lanes. The knots belonging to group 2, namely, k3, k4, k6, k7, k8, k15, and k17, are located in regions relatively free of dust, on the far side of the galaxy, and have lesser average extinction of $A_v = 1.63$. These knots lie in front of the outer dust ring as seen along the line of sight, unlike the knots belonging to group 1, which are seen through the outer dust ring. Group 3 consists of the nucleus k10 and two other circumnuclear knots, k13 and k14, and they have an average extinction of $A_v = 2.16$. The B/R color map also shows that the reddening in these regions is intermediate between that of group 1 and group 2. The colors of the star-forming knots were corrected for the average reddening obtained for the corresponding groups and then compared with model values.

For consistent values of colors and Hα equivalent widths, it is seen that the star-forming regions have ages less than 6.5 Myr, with the youngest of them being about 3.2 Myr. The nuclear starburst has an estimated age of 5.4 Myr. Also, the instantaneous star formation scenario can better accommodate the low Hα equivalent widths observed, as compared with the continuous star formation scenario, where the continuous availability of ionizing flux results in somewhat higher and nearly constant Balmer equivalent widths. The main uncertainty in the age estimation comes from the nonuniform reddening over the entire galaxy. A more precise understanding of the star formation scenario would require studies in the near-IR region and Brγ imaging, where the dust effects are less pronounced.

TABLE 4
Star Formation Rates for the Four Brightest H II Regions

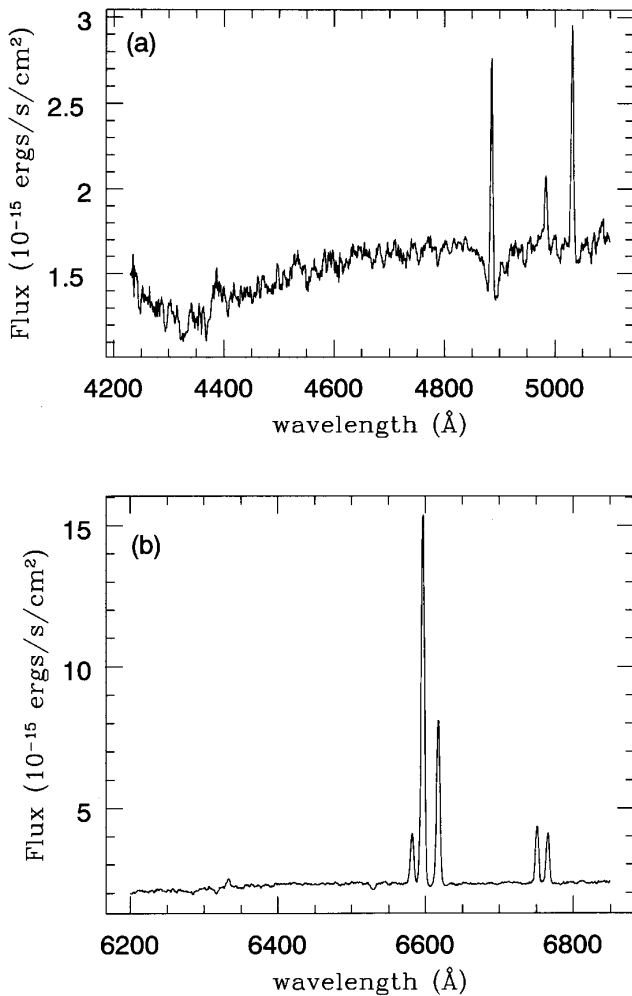| Region	Aperture Radius (pc)	SFR($\geq 10\ M_\odot$) ($M_\odot$ yr^{-1})	SFR(total) ($M_\odot$ yr^{-1})
k3	250	0.0163	0.102
k10	190	0.0519	0.325
k15	250	0.0733	0.459
k18	190	0.0227	0.142

FIG. 4.—Spectra of NGC 972: (a) the blue spectrum and (b) the red spectrum from Ho et al. (1995).

4.2. Emission-Line Diagnostics

We have used the spectra of NGC 972 from the optical spectral atlas for the nuclei of nearby galaxies compiled by Ho et al. (1995). The spectra were recorded using the double spectrograph on the 5 m Hale Telescope, which yielded simultaneous spectral coverage of the blue wavelength range 4230–5110 Å and the red wavelength range 6210–6860 Å. The spectral resolution obtained is 4 Å in the blue and 2.5 Å in the red. The blue and red spectra of NGC 972 are shown in Figure 4. The slit was oriented along the minor axis of the galaxy and the slit width was 2″, and the

TABLE 5

NUCLEAR EMISSION-LINE FLUXES

Line	Measured Flux[a] $(10^{-15}$ ergs s^{-1} cm$^{-2})$
Hβ	10.31
[O III] $\lambda5007$......	8.05
[O I] $\lambda6300$	2.04
Hα	79.73
[N II] $\lambda6583$	33.38
[S II] $\lambda6716$	12.27
[S II] $\lambda6731$	10.28

[a] Not corrected for reddening. See Ho et al. 1997 for more details on other emission lines.

spectra were extracted over apertures of 2″ × 4″, which corresponds to about 210 × 420 pc^2 at the distance of NGC 972. The nuclear spectrum is typical of starburst galaxies, with strong nebular emission lines arising from photoionization by massive stars. The fluxes measured for some of the important lines are given in Table 5.

In Table 6, we compare the emission-line ratios of NGC 972 with those of the well-known starburst galaxies M82 (NGC 3034), NGC 253, and NGC 1808. The table also contains emission-line ratios for the most prominent H II region in the starburst galaxy NGC 7552 (Forbes et al. 1994). From the table it is clear that the emission-line ratios for NGC 972 lie well within the range of values expected for starburst galaxies. The presence of low-ionization lines like [O I] $\lambda6300$ indicates that there is some amount of shock ionization. The [O I] $\lambda6300$/Hα ratio lies within the range of values seen in starburst galaxies that exhibit superwinds (Heckman, Armus, & Miley 1990; Armus, Heckman, & Miley 1989). Despite its relatively high inclination ($i = 65°$; Tully 1988), we do not see any extended emission in the Hα emission-line image of NGC 972 that is indicative of a superwind. Hence, it is probable that the supernova remnants (SNRs) present in the starburst region are responsible for the shock ionization giving rise to these low-ionization lines.

Diagnostic diagrams based on emission-line ratios are very useful for identifying the nature of ionization and for estimating the physical properties of the gaseous nebular emission in galaxies exhibiting spectra with strong emission lines. These diagrams help in classifying the nuclear spectra of galaxies as H II region–like or active galactic nucleus (AGN) like. When the nuclear emission-line ratios of NGC 972 are plotted on the diagnostic diagrams of Veilleux & Osterbrock (1987), it is evident that the ratios are slightly

TABLE 6

COMPARISON OF EMISSION-LINE RATIOS WITH OTHER STARBURST GALAXIES

Measured Ratio	NGC 972[a]	NGC 1808[b]	NGC 3034[c]	NGC 253[c]	NGC 7552[d]
log ([O III] $\lambda5007$/Hβ)................	−0.10	−0.60[e]	−0.46	...	−0.45
log ([N II] $\lambda6583$/Hα)................	−0.37	−0.07	−0.29	−0.11	−0.51
log ([S II] $\lambda\lambda(6717 + 6731)$/H$\alpha$)......	−0.54	−0.66	−0.62	−0.40	−0.58
log ([O I] $\lambda6300$/Hα)	−1.59	−1.88	−1.77	−1.36	−1.47
Hα/Hβ	7.7	15.0[f]	9.4	...	4.9

[a] L. C. Ho 1997, private communication.
[b] Phillips 1993.
[c] Armus et al. 1989.
[d] Forbes et al. 1994.
[e] Véron-Cetty & Véron 1986.
[f] Forbes, Boisson, & Ward 1992.

higher than expected for normal disk H II regions of spiral galaxies and lie in the region occupied by the prototypical starbursts.

H II nuclei including starbursts show stronger low-ionization forbidden line emission compared with normal disk H II regions (Kennicutt, Keel, & Blaha 1989; Ho et al. 1997). The possible explanations for the enhancement of low-ionization lines include (1) exceptionally hot stars that ionize the nebulae in the nuclear regions, where the physical conditions are likely to be different from disk regions, (2) shock ionization from SNRs, and (3) modification of the thermal properties of H II regions due to the presence of dust in high-metallicity environments. We have examined all these likely possibilities in the case of NGC 972.

In Figure 5, we indicate the positions occupied by the starburst regions given in Table 6 on emission-line ratio diagrams provided by C. Rola and collaborators (1997, private communication), in which new photoionization models have been used to demarcate the region occupied by H II region nuclei, which are powered by photoionization, from the AGNs, which are powered by massive black holes. These are dust-free, ionization-bounded models, which give the maximum boundary for gas that is photoionized by OB stars, corresponding to a large range in metallicity ($Z = 0.25$–2 $Z_{\odot}$), for $T_{eff} = 50,000$ K (*dashed lines*) and $T_{eff} = 60,000$ K (*solid lines*). The details of the models are

given in Tresse et al. (1996). Though it is difficult to make a clear distinction between the nuclear H II regions and starbursts, it is evident that both these classes tend to have slightly higher ratios compared with the normal disk H II regions and, hence, form an upper envelope of the position occupied by H II region–like objects. Knowing the [O III]/Hβ ratio for the nucleus, we estimated the metallicity using the empirical relation given by McCall, Rybski, & Shields (1985). We find that O/H for the nucleus is 1.9 times the solar value.

The nuclear spectroscopic data on NGC 972 reveal high metallicity ($Z = 2$ $Z_{\odot}$) and high extinction due to dust ($A_v = 2.8$). Shields & Kennicutt (1995) have studied the consequences of dust on the thermal properties of metal-rich H II regions, which are typical of starburst and H II nuclei. Their photoionization calculations show that in the presence of dust, the low-ionization lines are enhanced as a result of the increase in equilibrium electron temperature, mainly through depletion of gas-phase coolants. Using the diagnostic diagrams predicted by the above models that include the effects of dust, we find that the line ratios for NGC 972 lie well within the region occupied by starbursts and H II nuclei for the range $T_* = 38,000$–$45,000$ K. This does not require exceptionally hot stars as in the dust-free models. Thus it can be concluded that the nuclear emission-line spectrum of NGC 972 is a low-excitation spectrum
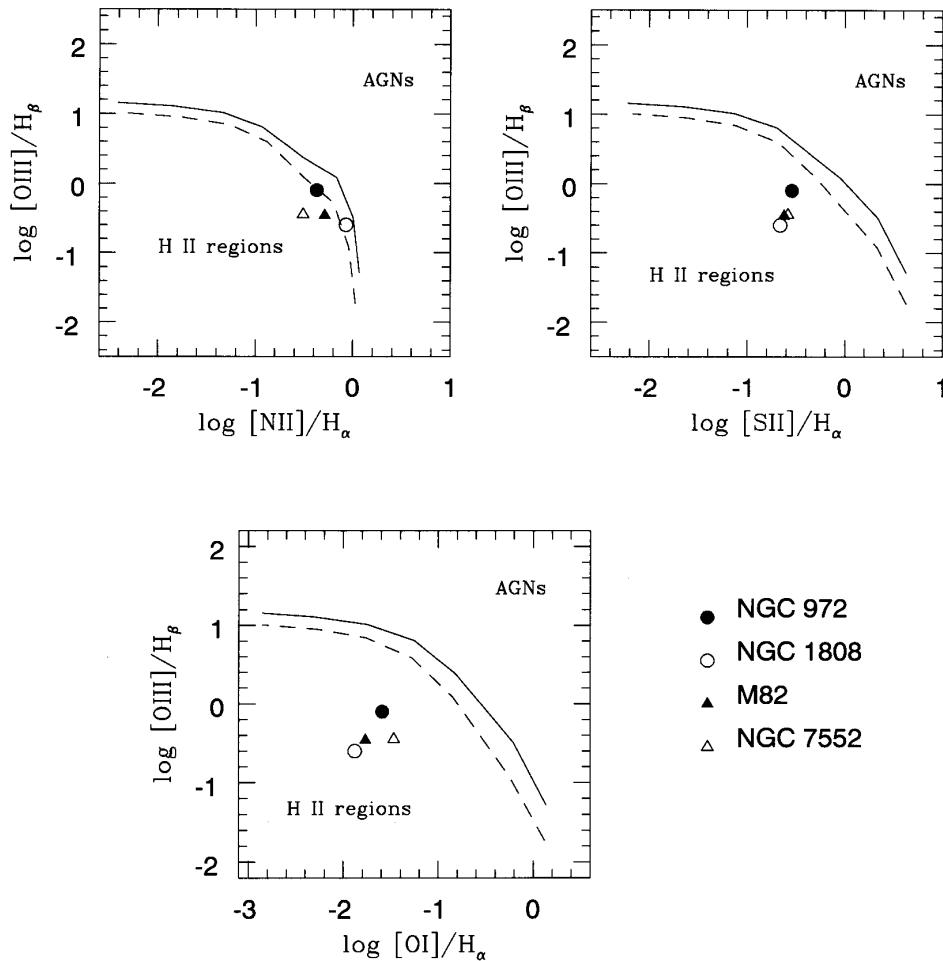

FIG. 5.—Diagnostic diagrams showing the positions occupied by starburst nuclei M82, NGC 1808, NGC 7552 (H II region), and NGC 972. The dashed and solid lines define the separation limits between AGNs and H II galaxies for $T_{eff} = 50,000$ and 60,000 K, respectively, based on the photoionization models of C. Rola (1997, private communication).

produced by photoionization due to massive stars in a high-metallicity environment, and having low-ionization lines enhanced because of the influence of dust.

As discussed by Forbes et al. (1994) for the case of NGC 7552, we examined the effects of shocks from SNRs on the line ratios. About a 20%–25% contribution from supernova shocks also appears to be a likely alternative to explain the enhancement of low-ionization lines.

4.3. Evidence for Starburst Activity and Possible Triggering Mechanisms

Most of the observational data available for NGC 972 are indicative of the presence of starburst activity in the nucleus. According to the classical definition (Balzano 1983), starburst nuclei have $H\alpha$ luminosities in the range 10^{40} to 10^{42} ergs s^{-1}. From our $H\alpha$ photometry, we obtain $L_{H\alpha} = 3.2 \times 10^{40}$ ergs s^{-1}, which is in good agreement with the value of 3.6×10^{40} ergs s^{-1} obtained by Ho et al. from their spectroscopic data. For comparison, the prototype starburst galaxy M82 has a nuclear $H\alpha$ luminosity of 1.6×10^{40} ergs s^{-1}. Starburst galaxies are characterized by high FIR luminosities and emit most of their bolometric luminosity in the 40–1000 μm range, peaking at 60 μm. The 40–120 μm luminosity is directly related to the SFR and is equal to 2.7×10^{10} $L_{\odot}$ (Devereux & Hameed 1997) in the case of NGC 972, which compares well to the $L(42–122\ \mu m)$ for the starburst galaxies M82 and NGC 253, being 2.32×10^{10} and 3.04×10^{10} $L_{\odot}$, respectively (Rice et al. 1988). The star formation rate obtained from the FIR luminosity using the conversion given by Devereux & Young (1991) amounts to 2.1 $M_{\odot}$ yr^{-1}. From our $H\alpha$ images we estimate an SFR of 2.7 $M_{\odot}$ yr^{-1} corresponding to the emission-line flux within an aperture of radius 36″ that encloses all the H II regions. The infrared-to-blue luminosity L_{IR}/L_B represents the ratio of recent, massive star formation to the average past star formation. The high value of $L_{IR}/L_B = 2.02$ in the case of NGC 972 is indicative of recent formation of massive stars. As discussed in the previous section, the emission-line ratios are also typical of starburst nuclei, with significant contributions from supernovae via shock heating.

One of the most interesting aspects of starburst phenomena has been to explain the triggering mechanisms that induce activity in these galaxies. Observations have shown that interacting galaxies have a higher rate of star formation compared with noninteracting galaxies (Lonsdale, Persson, & Matthews 1984; Hummel et al. 1990). Also, barred galaxies have a higher star formation rate than unbarred galaxies (Kennicutt et al. 1987; Hummel et al. 1990). Most ultraluminous $IRAS$ galaxies show tidal tails, double nuclei, and other such features that are evidence of recent merger activity (Sanders et al. 1988; Melnick & Mirabel 1990). Thus it appears that an interaction with another galaxy or the recent growth of a bar instability can act as a trigger for inducing activity in galaxies (see Phinney 1994 for a review). But NGC 972 appears to be an isolated galaxy that has no obvious signatures of interaction like tails or any other morphological distortions, and there is no evidence for a bar in the optical broadband images. Although the inner regions show a disturbed morphology, which is mainly due to the randomly distributed dust lanes, the outer isophotes appear undisturbed. In order to study the morphology in more detail and look for the presence of a bar, it would be necessary to rely on near-IR images, which are relatively transparent to dust. Preliminary analysis of the recently obtained near-IR images do not show very strong evidence for a dominant stellar bar (Mayya & Ravindranath 1997). However, the isophotal twists seen toward the central regions in the K band are suggestive of a weak barlike distortion.

Figure 1 of Vennick & Richter (1994) shows the NGC 972 group of galaxies, which contains seven spirals and irregular galaxies. The group also contains many dwarf spheroidals. Taniguchi (1986) suggested that the starburst activity may have been triggered by merging with a dwarf companion galaxy and that the dark dust lanes hold a key to the triggering mechanisms of the galaxy.

5. CONCLUSIONS

From BVR and $H\alpha$ photometry carried out on NGC 972, and the spectroscopic data available in the literature, we summarize the following results:

The continuum-subtracted $H\alpha$ emission-line image of NGC 972 indicates that most of the activity in this galaxy is concentrated within a radius of 3.4 kpc. The emission-line morphology reveals a circumnuclear ring of star-forming knots, with a break southeast of the nucleus. From the B/R color map a dust ring is found surrounding the nucleus, and this ring causes severe obscuration of the nucleus and circumnuclear star-forming regions.

The $H\alpha$ luminosities of the individual H II regions are comparable to that of GEHRs. The nucleus and the brightest disk H II region, which lies 16″ to the north of the nucleus, have luminosities that are typical of starbursts.

The emission-line ratios of NGC 972 are typical of starburst galaxies and agree with the spectra produced by photoionization due to massive stars in high-metallicity environments. The low-ionization emission lines are enhanced compared with the normal disk H II regions in spiral galaxies. The enhancement can be explained to be a result of the modification of the thermal properties of the nuclear H II regions by the influence of dust in high-metallicity environments. Some contribution from SNRs also appears to be a possible alternative to explain this enhancement of emission lines.

Using the evolutionary synthesis models of Mayya (1995), we estimate an age of less than 5.4 Myr for the nuclear starburst. The luminosities and colors are consistent with an instantaneous-burst model using Salpeter IMF with $M_{low} = 1$ $M_{\odot}$ and $M_{up} = 100$ $M_{\odot}$, assuming solar metallicity. The disk star-forming regions have colors and luminosities indicating an age less than 6.5 Myr. From the $H\alpha$ luminosity of the nucleus, we infer a star formation rate of 0.32 $M_{\odot}$ yr^{-1}.

The $H\alpha$ and IR luminosities over the inner 3.6 kpc radius indicate an SFR of 2.1–2.7 $M_{\odot}$ yr^{-1}. The high SFR, along with the high value of L_{IR}/L_B, shows that NGC 972 is a starburst galaxy.

REFERENCES

Andreasian, N. K., & Khachikian, E. E. 1979, Astrofizika, 15, 577 (English transl. Astrophysics, 15, 388 [1980])
Armus, L., Heckman, T. M., & Miley, G. 1989, ApJ, 347, 727
Balick, B., & Heckman, T. M. 1981, A&A, 96, 271
Balzano, V. 1983, ApJ, 268, 602
Burbidge, E. M., Burbidge, G. R., & Prendergast, K. H. 1965, ApJ, 142, 649
Calzetti, D., Kinney, A. L., & Storchi-Bergmann, T. 1994, ApJ, 429, 582
Cardelli, J. A., Clayton, G. C., & Mathis, J. S. 1989, ApJ, 345, 245
Condon, J. J., & Broderick, J. J. 1988, AJ, 96, 30
Conti, P. S. 1991, in Massive Stars in Starbursts, ed. C. Leitherer, N. R. Walborn, T. M. Heckman, & C. A. Norman (Cambridge: Cambridge Univ. Press), 21
Devereux, N., & Hameed, S. 1997, AJ, 113, 599
Devereux, N., & Young, J. S. 1991, ApJ, 371, 515
de Vaucouleurs, G., de Vaucouleurs, A., & Corwin, H. G., Jr. 1976, Second Reference Catalogue of Bright Galaxies (Austin: Univ. Texas Press)
de Vaucouleurs, G., de Vaucouleurs, A., Corwin, H. G., Jr., Buta, R. J., Paturel, G., & Fouqué, P. 1991, Third Reference Catalogue of Bright Galaxies (New York: Springer) (RC3)
Forbes, D. A., Boisson, C., & Ward, M. J. 1992, MNRAS, 259, 293
Forbes, D. A., Norris, R. P., Williger, G. M., & Smith, R. C. 1994, AJ, 107, 984
Heckman, T. M., Armus, L., & Miley, G. K. 1990, ApJS, 74, 833
Ho, L. C., Filippenko, A. V., & Sargent, W. L. W. 1995, ApJS, 98, 477
———. 1997, ApJ, 487, 579
Hodge, P. W., & Kennicutt, R. C., Jr. 1983, AJ, 88, 296
Hummel, E., van der Hulst, J. M., Kennicutt, R. C., & Keel, W. C. 1990, A&A, 236, 333
Keel, W. C. 1993, in ASP Conf. Ser. 35, Massive Stars: Their Lives in the Interstellar Medium, ed. J. P. Cassinelli & E. B. Churchwell (San Francisco: ASP), 498
Kennicutt, R. C., Jr. 1983, ApJ, 272, 54
———. 1988, ApJ, 334, 144
Kennicutt, R. C., Jr., Keel, W. C., & Blaha, C. A. 1989, AJ, 97, 1022

Kennicutt, R. C., Jr., Keel, W. C., van der Hulst, J. M., Hummel, E., & Roettiger, K. A. 1987, AJ, 93, 1011
Landolt, A. U. 1992, AJ, 104, 340
Longo, G., & de Vaucouleurs, A. 1983, General Catalogue of Photoelectric Magnitudes and Colors of Galaxies (Austin: Dept. Astron., Univ. Texas)
Lonsdale, C. J., Persson, S. E., & Matthews, K. 1984, ApJ, 287, 95
Massey, P., Strobel, K., Barnes, J. V., & Anderson, E. 1988, ApJ, 328, 315
Mayya, Y. D. 1995, AJ, 109, 2503
Mayya, Y. D., & Prabhu, T. P. 1996, AJ, 111, 1252
Mayya, Y. D., & Ravindranath, S. 1997, in preparation
McCall, M. L., Rybski, P. M., & Shields, G. A. 1985, ApJS, 57, 1
Melnick, J., & Mirabel, I. F. 1990, A&A, 231, L19
Phillips, A. 1993, AJ, 105, 486
Phinney, E. S. 1994, in Mass-Transfer Induced Activity in Galaxies, ed. I. Shlosman (Cambridge: Cambridge Univ. Press), 1
Rice, W., Lonsdale, C. J., Soifer, B. T., Neugebauer, G., Koplan, E. L., Lloyd, L. A., de Jong, T., & Habing, H. J. 1988, ApJS, 68, 91
Roberts, M. S. 1969, AJ, 74, 859
Sandage, A., & Tammann, G. A. 1987, A Revised Shapley-Ames Catalog of Bright Galaxies (2d ed.; Washington: Carnegie Inst. Washington)
Sanders, D. B., Soifer, B. T., Elias, J. H., Madore, B. F., Matthews, K., Neugebauer, G., & Scoville, N. Z. 1988, ApJ, 325, 74
Shields, J. C., & Kennicutt, R. C., Jr. 1995, ApJ, 454, 807
Spinoglio, L., & Malkan, M. A. 1989, ApJ, 342, 83
Taniguchi, Y. 1986, PASJ, 38, 571
Tresse, L., Rola, C., Hammer, F., Stasińska, G., Le Fèvre, O., Lilly, S. J., & Crampton, D. 1996, MNRAS, 281, 847
Tully, R. B. 1988, Nearby Galaxies Catalog (Cambridge: Cambridge Univ. Press)
Veilleux, S., & Osterbrock, D. E. 1987, ApJS, 63, 295
Vennick, J., & Richter, G. M. 1994, Astron. Nachr., 315, 245
Véron-Cetty, M.-P., & Véron, P. 1986, A&AS, 66, 335
Waller, W. H. 1990, PASP, 102, 1217
Young, J. S., Xi, S., Kenney, J. D. P., & Rice, W. L. 1989, ApJS, 70, 699